Model for Studying Unsteady Droplet Combustion

Josette Bellan* and Martin Summerfield†
Princeton University, Princeton, N.J.

The concept of a reduced boundary condition at the surface of a droplet is used to develop a theory of unsteady droplet burning. This theory utilizes a quasi-steady gas-phase assumption, which has been shown to be realistic for a wide range of droplet sizes at low pressures. The most significant consequence of the theory is that the problem of unsteady droplet burning is reduced to the solving of a *single* diffusion-type nonlinear partial differential equation having one of its boundary conditions determined by an algebraic function of the quasi-steady gas-phase variables. This reduced boundary condition incorporates the entire dependence of the solution on fuel characteristics, chemical kinetics, and thermal properties of the gases. An experiment is proposed for determining this boundary condition so that the nonsteady droplet combustion problem can be solved for a realistic situation. By using additional assumptions, a numerical estimate of the boundary condition has been made.

Nomenclature

A = preexponential constant in the Arrhenius law, cm^3/mole-sec
B_i = function of dimensional variables
C = constant proportional to the heat of combustion, cal/g
c_1, c_2 = nondimensional constants
C_p = total heat capacity at constant pressure, cal/g-K
C_{pi} = heat capacity at constant pressure for species i, cal/g-K
D = diffusivity, cm^2/sec
E = activation energy, cal/mole
$\hat{F}_1, \hat{F}_2$ = functions of dimensional temperatures and temperature gradients
F_1, F_2 = functions of nondimensional temperatures and temperature gradients
G = $\dot{m}/4\pi$, g/sec
h_i^0 = specific formation enthalpy for species i, cal/g
L_{dg} = heat of evaporation, cal/mole
Le = Lewis number
$\dot{m}$ = mass evaporation rate, g/sec
N = stoichiometric number of moles
p = pressure, atm
p_c = pressure, cal/cm^3
Q_s = heat evolved at the surface of the droplet, cal/g
r = radial coordinate, cm
R = radius of the droplet, cm
$\tilde{R}$ = gas constant, cal/g-K
R_u = universal gas constant; $R_u = 1.986$ cal/mole-K
$\hat{R}_u$ = universal gas constant; $\hat{R}_u = 0.81 \times 10^{-4}$ $atm\,cm^2\,sec^2$/g-mole-K
$\hat{S}_1, \hat{S}_2$ = functions of dimensional temperatures and temperature gradients
S_1, S_2 = functions of nondimensional temperatures and temperature gradients
T = temperature, K
W_i = molecular weight of species i, g/mole
y = nondimensional variable, r/R
Y_i = mass fraction for species i
α = overall evaporation coefficient in the Langmuir-Knudsen law
Γ_i = Shvab-Zeldovich or Shvab-Zeldovich-like variable
$\Delta r_{\min}$ = minimum thickness of a thermal layer, cm
θ = nondimensional temperature, T/T_{ref}
λ = coefficient of heat conductivity, cal/cm-K-sec
μ = gas viscosity, g/cm-sec
ρ = density, g/cm^3
ϕ = $\partial T/\partial r$, K/cm

Subscripts

b = boiling point
d = droplet
F = fuel
g = gas
N = N_2
O = O_2
P = products
ref = reference
s = at the surface of the droplet
∞ = at infinity

Superscripts

ss = steady-state

Notations

$| \; |$ = absolute value

Introduction

THE nonsteady nature of burning droplets is clearly reflected by the time variation of the ratio of droplet diameter to flame diameter during the major part of the droplet lifetime.[1] Even though the quasi-steady theory is able to predict fairly well the droplet diameter during combustion by the d^2 law,[2] many properties, including the heat and mass transfer in the gas and liquid phase, are in a transient state and, therefore, cannot be determined from this theory. The situation becomes critical especially in problems where inherently nonsteady information is required. Such problems occur in explosions through sprays, rocket engines subject to combustion instabilities, and studies of extinction and ignition. All these problems are of practical importance and have stimulated efforts to develop a detailed theory of nonsteady burning.

As early as 1959, Spalding[3] proposed a theoretical model for droplet combustion. More work in this area was done by Strahle[4] and Chervinsky.[5] Kotake and Okazaki[6] solved numerically the unsteady evaporation and combustion problem. However, Hubbard et al.[7] pointed out that the results of Ref. 6 were not in agreement with experiments. In Ref. 7, new numerical results were presented for the

Received July 1, 1975; presented as Paper 76-614 at the AIAA/SAE 12th Propulsion Conference, Palo Alto, Calif., July 26-29, 1976; revision received Oct. 6, 1976.

Index categories: Combustion in Heterogeneous Media; Combustion Stability, Ignition, and Detonation; Reactive Flows.

*Member of Professional Staff. Member AIAA.
†Professor. Fellow AIAA.

evaporation problem and good agreement with experiments was obtained. Other investigators[2,8] attempted to use experimental correlations to incorporate in the solution the unsteady characteristics of the burning of a droplet while still maintaining the quasi-steady aspect of the solution. All the above models are limited by the following difficulties: there is a lack of knowledge about the chemical mechanisms and kinetics for the majority of fuels; the equations are generally difficult to integrate because of additional nonlinearities introduced by $C_{pi}(T)$, $\lambda(Y_i,T)$, $\mu(Y_i,T)$; finally the facts that the diffusion coefficients depend on the species, and for realistic situations $Le \neq 1$, make the problem even more cumbersome.

The well-known steady-state solution with no penetration of oxygen at the droplet surface[9] predicts no dependence of $\dot{m}$ upon p except through the evaporation law. In reality, the chemical kinetics effect of p on $\dot{m}$ may be important for small droplets burning at low pressures. Tarifa[10] pointed out that the errors introduced by disregarding the finite kinetics could be of consequence in many practical cases. For this reason, this work does not assume a thin flame in the gas phase.

In this paper, a genuine nonsteady theory is presented. This theory, combined with data from a proposed experiment, precludes the need for chemical kinetic information. The data also implicitly account for the variation of C_p, λ, and μ with T and Y_i, for the fact that the diffusion coefficients are not equal for all species, and for the fact that $Le \neq 1$.

The present study is inspired by Zeldovich's work[11,12] on unsteady solid-propellant burning. Following his approach the objective is to find a convenient functional form for the boundary condition associated with the unsteady energy equation in the liquid phase. This boundary condition should satisfy several criteria; it should have a unique functional form for all problems, and it should include all the effects of the gas phase upon the burning droplet. Also, the numerical values of this boundary condition should be determinable from simple experiments. Then, once this boundary condition is obtained, the knowledge of the detailed structure of the flame in the gas field is unnecessary for solving all single droplet burning problems.

Theoretical Model for Unsteady Droplet Burning

Assumptions

1) There is no natural or forced convection of gases from regions far from the droplet. It is well known that the size of the fuel droplets in actual engines is smaller by one order of magnitude than that of droplets used in laboratory experiments.[9] For the former type of droplets, the influence of natural convective flow is negligible,[6] whereas the influence of a forced convective flow can be obtained by using correlations[9] between the mass burning rates with and without convection.

2) All dependent variables in the problem are spherically symmetric. (Note that this is consistent with Assumption 1.)

3) The burning in the gas phase occurs in a quasi-steady manner. For the droplet sizes of interest, and for the range of low pressures considered here, this is a very realistic assumption.[13]

4) The evaporation occurs only from the surface of the droplet rather than from a more realistic zone of finite thickness at the surface. As a consequence of this assumption, no reactions occur in the liquid phase. By making this assumption, the very short characteristic response time of the finite thickness layer in which chemical reactions and ultimately the evaporation occurs is ignored.

5) Gravity effects are ignored. For the large droplets used in experiments, gravity causes slight distortion from spherical symmetry, whereas for small droplets, such as those in engines, this effect is negligible.[6]

6) The temperature is continuous at the droplet surface.

7) Radiative heat transfer is neglected.

8) The Mach number of the gases in the system is less than unity and small. As a consequence, one can deduce from the momentum equation that the pressure is a function of time only. Moreover, in the energy equation, the kinetic energy and viscous dissipation terms may be neglected when compared to the other terms.

9) Since the actual chemical kinetic steps of the reaction between fuel in the gas phase and oxygen are not known, the following one-step reaction is assumed, but can be easily relaxed:

$$F + N_O O_2 + 3.76 N_O N_2 \rightarrow N_P P + 3.76\, N_O N_2$$

The following assumptions frequently used in theories of droplet combustion will not be made here

$Le = 1$.
The diffusion coefficients are equal for all species.
ρD is a constant.
λ and C_p are constants.

Existence of Two Unique Functions Summarizing the Effect of the Gas Phase on the Droplet

The objective is to find a way of expressing the influence of the gas phase on the liquid phase in a simple manner. It is convenient to imagine that the gas phase acts as a "boundary condition" at the surface of the droplet and the liquid phase responds to it accordingly. With this image in mind, a reduced boundary condition for the unsteady energy equation of the droplet can be derived. The term "reduced" implies that there is a minimum number of variables present in the boundary condition; the other variables have been eliminated using independent relationships. These relationships are listed below in their functional forms.

1) The energy balance at the droplet surface

$$B_1(\phi_{ds}, \phi_{gs}, \dot{m}, R, T_{gs}, T_{ds}) = 0 \tag{1}$$

2) The Langmuir-Knudsen evaporation law

$$B_2(\dot{m}, R, p, T_{gs}, T_{ds}, Y_{Fs}, Y_{Os}, Y_{Ps}, Y_{Ns}) = 0 \tag{2}$$

3) Continuity of temperature at the droplet surface

$$B_3(T_{ds}, T_{gs}) = 0 \tag{3}$$

4) Balance of fluxes of fuel at the droplet surface

$$B_4\left(\dot{m}, R, Y_{Fs}, \frac{dY_F}{dr}\Big)_s\right) = 0 \tag{4}$$

5) Balance of fluxes of oxygen at the droplet surface

$$B_5\left(\dot{m}, R, Y_{Os}, \frac{dY_O}{dr}\Big)_s\right) = 0 \tag{5}$$

6) Balance of fluxes of nitrogen at the droplet surface

$$B_6\left(\dot{m}, R, Y_{Ns}, \frac{dY_N}{dr}\Big)_s\right) = 0 \tag{6}$$

7) Balance of fluxes of products at the droplet surface

$$B_7\left(\dot{m}, R, Y_{Ps}, \frac{dY_P}{dr}\Big)_s\right) = 0 \tag{7}$$

8) If a Shvab-Zeldovich-like variable is $\Gamma_1 = C_{pg}T_g/C + Y_F/c_1$, then a formal solution for Γ_1 satisfying the boundary conditions at the droplet surface and at infinity can

be expressed in a functional form. Computing formally $d\Gamma_1/dr$ and evaluating it at the droplet surface yields

$$B_8\left(\dot{m},R,T_\infty,T_{gs},Y_{F\infty},Y_{Fs},\phi_{gs},\frac{dY_F}{dr}\right)_s,Y_{Ps},Y_{P\infty},\frac{dY_P}{dr}\Big)_s$$

$$Y_{O\infty},Y_{Os},\frac{dY_O}{dr}\Big)_s,Y_{Ns},Y_{N\infty},\frac{dY_N}{dr}\Big)_s\Big)=0 \tag{8}$$

9) The previous procedure can be repeated for $\Gamma_2=Y_F/c_1-Y_O$. Another function is obtained

$$B_9\left(\dot{m},R,Y_{F\infty},Y_{O\infty},T_\infty,Y_{Fs},Y_{Os},T_{gs},\frac{dY_F}{dr}\right)_s \quad \frac{dY_O}{dr}\Big)_s,\phi_{gs}\Big)=0 \tag{9}$$

10) Again, the procedure can be applied to $\Gamma_3=Y_P/c_2+Y_O$. The function obtained is

$$B_{10}\left(\dot{m},R,Y_{P\infty},Y_{O\infty},T_\infty,T_{Ps},Y_{Os},T_{gs},\frac{dY_P}{dr}\right)_s,\frac{dY_O}{dr}\Big)_s,\phi_{gs}\Big)=0 \tag{10}$$

11) Once more, the procedure can be used for Y_N to yield

$$B_{11}\left(\dot{m},R,Y_{N\infty},Y_{Ns},\frac{dY_N}{dr}\right)_s,T_\infty,T_{gs},\phi_{gs}\Big)=0 \tag{11}$$

12) The variable T_g is not a Shvab-Zeldovich-like variable because it satisfies a nonhomogeneous equation. However, the procedure for finding Eq. (8) can be repeated again to yield the formal relation

$$B_{12}\left(\dot{m},R,p,T_{gs},\phi_{gs},Y_{Fs},Y_{Os},Y_{Ps},Y_{Ns},\frac{dY_F}{dr}\right)_s,\frac{dY_O}{dr}\Big)_s,$$

$$\frac{dY_P}{dr}\Big)_s,\frac{dY_N}{dr}\Big)_s,T_\infty,Y_{F\infty},Y_{O\infty},Y_{N\infty},Y_{P\infty};$$

$$\text{chemical kinetics}\Big)=0 \tag{12}$$

13) Conservation of mass at infinity

$$B_{13}(Y_{O\infty},Y_{F\infty},Y_{N\infty},Y_{P\infty})=0 \tag{13}$$

The previous set of equations contains the following 20 variables

$\dot{m},R,p$	3
$T_{gs},T_{ds},\phi_{gs},\phi_{ds}$	4
$Y_{Fs},Y_{Os},Y_{Ps},Y_{Ns},\frac{dY_F}{dr}\Big)_s,\frac{dY_O}{dr}\Big)_s,\frac{dY_N}{dr}\Big)_s,\frac{dY_P}{dr}\Big)_s$	8
$T_\infty,Y_{F\infty},Y_{O\infty},Y_{P\infty},Y_{N\infty}$	5
	20

This set of 13 equations and 20 variables can be reduced to one equation containing eight variables. Let it be

$$\hat{F}_1(\dot{m},R,p,\phi_{ds};\ T_\infty,Y_{O\infty},Y_{F\infty},Y_{N\infty};\ \text{chemical kinetics})=0 \tag{14}$$

The "reduced" boundary condition at the droplet surface is found by formally solving Eq. (14) for ϕ_{ds}

$$\phi_{ds}=\hat{S}_1(\dot{m},R,p;\ T_\infty,Y_{O\infty},T_{F\infty},Y_{N\infty};\ \text{chemical kinetics}) \tag{15}$$

Notice now that Eq. (15) is insufficient for summarizing the behavior of the gas phase. Indeed, suppose that for a given droplet (R known), at a certain pressure and imposed conditions at infinity, one would like to find ϕ_{ds}. Equation (15) does not provide the answer because $\dot{m}$ is unknown. Therefore, another function is necessary to complete the information provided by Eq. (15).

The previous system of 13 equations and 20 unknowns can be reduced in another way to yield again an equation containing eight variables

$$\hat{F}_2(\dot{m},R,p,T_{ds};\ T_\infty,Y_{O\infty},Y_{F\infty},Y_{N\infty};\ \text{chemical kinetics})=0 \tag{16}$$

Solving Eq. (16) for $\dot{m}$ one obtains

$$\dot{m}=\hat{S}_2(R,p,T_{ds};\ T_\infty,Y_{O\infty},Y_{F\infty},Y_{N\infty};\ \text{chemical kinetics}) \tag{17}$$

Now, either in the case of the steady-state droplet burning at a given surface temperature or in the case of the unsteady droplet burning (when initial conditions give the temperature profile inside the droplet), the quantity T_{ds} is known. Then, through $\hat{S}_2$ one can find $\dot{m}$ (which indicates the regression rate of the droplet). Once $\dot{m}$ is known, $\hat{S}_1$ gives ϕ_{ds}.

Experimental Method for Determining the Two Functions

A very important feature of functions $\hat{F}_1$ and $\hat{F}_2$ (or $\hat{S}_1$ and $\hat{S}_2$) is that they are unique for a given fuel. Indeed, in the theoretical derivation, no information regarding the liquid

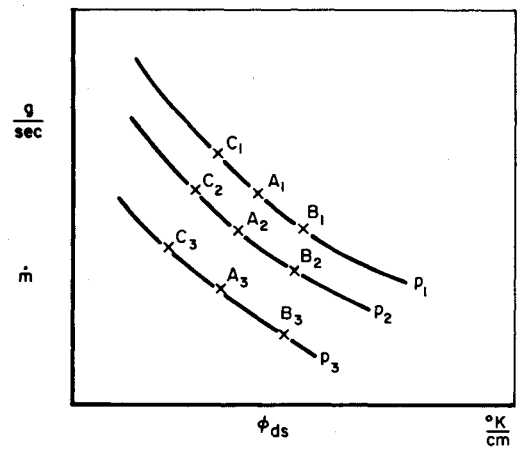

Fig. 1 Sketch of a hypothetical function $\hat{S}_1$ for a given fuel. The conditions at infinity are fixed and so is R.

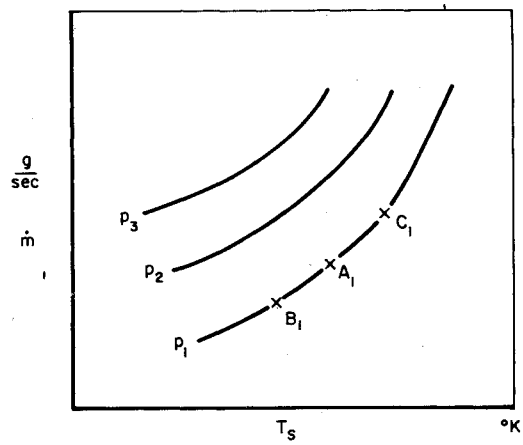

Fig. 2 Sketch of a hypothetical function $\hat{S}_2$ for a given fuel. The conditions at infinity are fixed and so is R.

phase was used; it could be steady or unsteady. Then, because of their uniqueness, $\hat{F}_1$ and $\hat{F}_2$ (or $\hat{S}_1$ and $\hat{S}_2$) can be determined from steady-state experiments. Once a multidimensional map is available for each one of the functions, then because of the uniqueness of these functions, the maps can be used in steady-state or unsteady combustion problems. If a steady-state energy equation is solved for the droplet in association with the two functions, the solution of a steady-state problem is found; if the two functions are associated with an unsteady energy equation, the solution of an unsteady problem is found.

There are several advantages in determining the two functions experimentally rather than numerically. First, notice that knowledge of $\hat{F}_1$ and $\hat{F}_2$ eliminates the need for information on chemical mechanisms and chemical kinetics; if no chemical kinetic measurement is to be performed, this already presents a great advantage. Second, no assumptions have to be made regarding the variation of the thermochemical quantities; their influence is imbedded into $\hat{F}_1$ and $\hat{F}_2$. Third, the real variation of the diffusion coefficients for different species is also accounted for in $\hat{F}_1$ and $\hat{F}_2$.

The set of measurements proposed here can be performed with the classical porous surface droplet fed with fuel in its center so that a steady-state condition is maintained. The sequence of measurements is as follows.

1) Fix the conditions at infinity, p and R.

2) Measure $\dot{m}$ (i.e., the quantity of mass per unit time needed to maintain the steady-state situation).

3) Measure $T_d(r=0)$ with a thermocouple.

4) Measure T_{ds} with a thermocouple. (Appendix A elaborates on the errors of such a measurement.) Since $\dot{m}$ and T_{ds} are known, a point A_1 is obtained on the graph in Fig. 2 representing schematically $\hat{S}_2$.

5) Find ϕ_{ds} from the steady-state energy equation of the droplet:

$$\phi_{ds}^{ss} = \frac{\dot{m}^{ss}}{4\pi R^2 \lambda_d} C_{pd}\left[T_{ds}^{ss} - T_d^{ss}(r=0)\right]$$

The quantities C_{pd} and λ_d can be obtained from tables on thermochemical data.[1] A point A_1 has now been obtained on the graph in Fig. 1 representing schematically $\hat{S}_1$.

6) In order to obtain another point on the graph (i.e., another measurement at the same pressure), $T_d^{ss}(r=0)$ can be changed. At the point B_1 on both graphs $T_d^{ss}(r=0)$ is lower; at the point C_1, $T_d^{ss}(r=0)$ is higher. The sequence of measurements 2-5 must be performed again for each $T_d^{ss}(r=0)$. Since the droplet is now fed with fuel at different temperatures, the completion of the measurements for one curve (at a fixed pressure) depends on the ability to vary $T_d^{ss}(r=0)$. It should be recognized that there are difficulties on dropping $T_d^{ss}(r=0)$ beyond certain levels, and thus of obtaining measurements for very low values of $\dot{m}$.

7) In order to obtain the maps of Figs. 1 and 2, the pressure is varied and steps 2-6 are repeated.

8) By varying R and going through steps 2-7, one can complete the map in another dimension.

9) A multidimensional map may be obtained by varying the conditions at infinity and by repeating for each set of conditions steps 2-8.

Numerical Experiments

The purpose of the numerical experiments is to determine the functions S_1 and S_2 from calculations rather than from experiments. It is realized that in this way the advantage of not requiring chemical kinetics information and that of having a rather unrestricted set of assumptions is lost. However, it is considered that this is a worthwhile way of obtaining these two functions and showing their behavior. For this purpose the additional assumptions mentioned at the end of the subsection entitled "Assumptions," but not used in the general theory are adopted. The computation is performed for decane droplets.

Equations and Method of Solution

Preliminary Relationships

a) A general solution of the nondimensional homogeneous diffusion equation with imposed boundary conditions at $y=1$ and $y\to\infty$ is

$$\Gamma_i(y) = \frac{(\Gamma_{i\infty} - \Gamma_{is})\exp\left(-\frac{GC_{pg}}{\lambda_g R}\frac{1}{y}\right) + \Gamma_{is} - \Gamma_{i\infty}\exp\left(-\frac{GC_{pg}}{\lambda_g R}\right)}{\left[1-\exp\left(-\frac{GC_{pg}}{\lambda_g R}\right)\right]} \tag{18}$$

Using Eq. (18) (for Γ_1, Γ_2, Γ_3, and Y_N) and the boundary conditions on the mass fractions at the surface of the droplet[9] one may obtain the following relationships

$$\frac{Y_{Fs}}{c_1} - Y_{Os} - \frac{1}{c_1} = \left(\frac{Y_{F\infty}}{c_1} - Y_{O\infty} - \frac{1}{c_1}\right)\exp\left(-\frac{GC_{pg}}{\lambda_g R}\right) \tag{19}$$

$$\frac{Y_{Ps}}{c_2} + Y_{Os} = \left(\frac{Y_{P\infty}}{c_2} + Y_{O\infty}\right)\exp\left(-\frac{GC_{pg}}{\lambda_g R}\right) \tag{20}$$

$$Y_{Ns} = Y_{N\infty}\exp\left(-\frac{GC_{pg}}{\lambda_g R}\right) \tag{21}$$

$$\left(\frac{d\theta_g}{dy}\right)_s = \frac{GC_{pg}}{\lambda_g R}\exp\left(-\frac{GC_{pg}}{\lambda_g R}\right) \times\left[\frac{(\theta_\infty - \theta_s) + \frac{C}{C_{pg}T_{ref}}\frac{Y_{F\infty}-Y_{Fs}}{c_1}}{1-\exp\left(-\frac{GC_{pg}}{\lambda_g R}\right)}\right] - \frac{GC_{pg}}{\lambda_g R}\frac{C}{C_{pg}T_{ref}}(Y_{Fs}-1) \tag{22}$$

where

$$c_1 = \frac{W_F}{W_O}\frac{1}{N_O} \qquad c_2 = \frac{W_P}{W_O}\frac{N_P}{N_O} \qquad C = c_1 h_F^Q - c_2 h_P^Q$$

b) From the Langmuir-Knudsen relationship

$$G = \alpha R^2\left\{p\exp\left[\frac{L_{dg}}{R_u T_{ref}}\left(\frac{1}{\theta_b}-\frac{1}{\theta_s}\right)\right] - \frac{Y_{Fs}}{W_F}\frac{R_u}{\tilde{R}}p\right\}\left(\frac{W_F}{2\pi\hat{R}_u\theta_s T_{ref}}\right)^{1/2} \tag{23}$$

and Eqs. (19-21) the following expression is obtained

$$Y_{Fs} = \left\{\left[\exp\left(-\frac{GC_{pg}}{\lambda_g R}\right)-1\right]\times\left[\frac{W_F}{W_O} - c_2\frac{W_F}{W_P}\right]\Big/c_1 + \exp\left(-\frac{GC_{pg}}{\lambda_g R}\right)\times\left[-\frac{Y_{F\infty}}{c_1}\left(\frac{W_F}{W_O} - c_2\frac{W_F}{W_P}\right) + Y_{O\infty}\frac{W_F}{W_O} + Y_{P\infty}\frac{W_F}{W_P} + Y_{N\infty}\frac{W_F}{W_N}\right]\right\}\Big/\left[1/FCN - \left(1 + \frac{W_F}{c_1 W_O} - \frac{c_2 W_F}{c_1 W_P}\right)\right] \tag{24}$$

where

$$FCN=\exp\left[\frac{L_{dg}}{R_u T_{\text{ref}}}\left(\frac{1}{\theta_b}-\frac{1}{\theta_s}\right)\right]$$

$$-\frac{G}{\alpha R^2 p}\frac{1}{[W_F/(2\pi\tilde{R}_u T_{\text{ref}}\theta_s)]^{1/2}}$$

Method of Solution

Using a Shvab-Zeldovich formulation[9] for thick diffusion flames, it is found that among all independent differential equations describing the problem, only one is nonhomogeneous and, therefore, has to be solved numerically. Here the choice has been made to numerically solve the equation for the fuel mass fraction, namely

$$\frac{d^2 Y_F}{dy^2}-\left[\frac{GC_{pg}}{\lambda_g R}\frac{1}{y^2}-\frac{2}{y}\right]\frac{dY_F}{dy}$$

$$-\frac{A\exp[-E/(R_u T_{\text{ref}}\theta)]}{W_F}c_1 Y_O Y_F$$

$$\times\left(\frac{p_c}{\tilde{R}T_{\text{ref}}}\frac{1}{\theta}\right)^2\frac{C_{pg}R^2}{\lambda_g}=0 \qquad (25)$$

where

$$\tilde{R}=R_u\sum_i\frac{Y_i}{W_i} \qquad i=F,O,N,P$$

The algebraic equations used with it are

$$\theta=[\Gamma_1-(Y_F/c_1)][C/(C_{pg}T_{\text{ref}})] \qquad (26)$$

where Γ_1 is given by Eq. (18),

$$Y_O=(Y_F/c_1)-\Gamma_2 \qquad (27)$$

where Γ_2 is given by Eq. (18),

$$Y_N, \text{ given by Eq. (18)}, \qquad (28)$$

$$Y_P=1-Y_F-Y_O-Y_N \qquad (29)$$

The rationale of the computation is the following. Suppose that a given droplet of radius R burns in a given environment (i.e., given conditions at infinity) at a pressure p. For this situation, the graphs equivalent to those in Figs. 1 and 2 will be obtained here by varying $(\partial\theta_d/\partial y)_s$. The following shows how one obtains a point on each curve. (Note that a point on the curve represents a quasi-steady solution of the gas field.)

For fixed p and $(\partial\theta_d/\partial y)_s$ a quasi-steady solution is calculated by a trial and error procedure with G being the eigenvalue.[14,15] The first step consists of choosing G and computing θ_s such that the value of $(d\theta_g/dy)_s$ given by Eq. (22) (via Eq. 24) corresponds to the value given by the boundary condition of the energy equation, namely

$$\left(\frac{d\theta_g}{dy}\right)_s=\frac{G}{\lambda_g R T_{\text{ref}}}\left[Q_s+\frac{\lambda_d R T_{\text{ref}}}{G}\left(\frac{\partial\theta_d}{\partial y}\right)_s\right] \qquad (30)$$

(Q_s is taken here as the heat of vaporization since the heat capacities of the liquid and gas phase are considered equal at the droplet surface. The value of Q_s is constant for all computations at a fixed pressure and taken as that obtained for θ_b. An average value of λ_g and C_{pg} is used, and the value of λ_d is that corresponding to θ_s for the solution obtained with $(\partial\theta_d/\partial y)_s=0$. In all the computations $\alpha=1$.) Once θ_s is known, Y_{Fs} is computed from Eq. (24). Then Y_{Os} and Y_{Ps} follow from Eqs. (19) and (20). Y_{Ns} is computed from Eq. (21). With these boundary conditions the integration of Eq. (25) is performed by a Runge-Kutta method. Equations (26-29) give the values of the other dependent variables at any point y once Y_F is known there. The criterion for recognizing a quasi-steady solution is presented in Appendix B. The thermochemical data used in the computation are taken from Ref. 16.

Results for a Given R, θ_∞, *and Ambient Gas Composition*

Figures 3 and 4 show the results equivalent to the schematic drawings of Figs. 1 and 2. It is first interesting to interpret the results obtained for a fixed pressure. For that purpose the results obtained varying $(\partial\theta_d/\partial y)_s$ are compared. The results for $p=10$ atm are presented in Table 1; these constitute the reference case.

Whenever $(\partial\theta_d/\partial y)_s$ is negative, the droplet is hot enough so that it is able to give off heat. (Notice that the heat goes only into the surface since $(d\theta_g/dy)_s$ is always positive when there is burning in the gas field.) Since the droplet is now hotter than when the condition $(\partial\theta_d/\partial y)_s=0$ prevailed (when it

Table 1 Quasi-steady gas-phase solutions for the reference case[a]

$\left(\frac{\partial\theta_d}{\partial y}\right)_s$	−5 (−79° angle)	−4 (−76° angle)	−1 (−45° angle)	0 (0° angle)	1 (+45° angle)	5 (+79° angle)
$G\times10^5$ g/sec	There is	3.920302525	1.98472273	1.61998	1.3326197	0.4983
$\frac{GC_{pg}}{\lambda_g R}$	no quasi-steady solution	6.751634	3.4181345	2.78996	2.295068	0.85818
$\left(\frac{d\theta_g}{dy}\right)_s$		0.06058459	0.894389	1.41777	2.0088695	4.6490632
	with	(3.47° angle)	(41.81° angle)	(54.80° angle)	(63.54° angle)	(77.86° angle)
θ_s	$\theta_s<\theta_b$	1.897769 (565.53 K)	1.84281 (549.16 K)	1.79935 (536.21 K)	1.746844 (520.56 K)	1.458393 (434.60 K)
Y_{Fs}		0.998753	0.9650394	0.934478	0.8925264	0.5502393
Y_{Os}		0.1752 $\times10^{-8}$	0.7404366 $\times10^{-7}$	0.124362 $\times10^{-5}$	0.1682961 $\times10^{-4}$	0.8598342 $\times10^{-2}$
Y_{Ps}		0.350495 $\times10^{-3}$	0.982654 $\times10^{-2}$	0.184152 $\times10^{-1}$	0.301880 $\times10^{-1}$	0.116049
Y_{Ns}		0.896484 $\times10^{-3}$	0.25134 $\times10^{-1}$	0.471056 $\times10^{-1}$	0.772687 $\times10^{-1}$	0.325113

[a] $p=10$ atm; $T_b=566$ K; $R=10^{-2}$ cm; $Y_{F\infty}=Y_{P\infty}=0$; $Y_{O\infty}=0.2331$; $Y_{N\infty}=0.7669$; $T_\infty=298$ K; $A=1.382\times10^{12}$ cm^3/mole sec; $E=40$ kcal/mole; $L_{dg}=6000$ cal/mole; $Q_s=42.25$ cal/g; $\lambda_{\text{liquid decane at 536 K}}=0.1365\times10^{-3}$ cal/sec-cm-K.

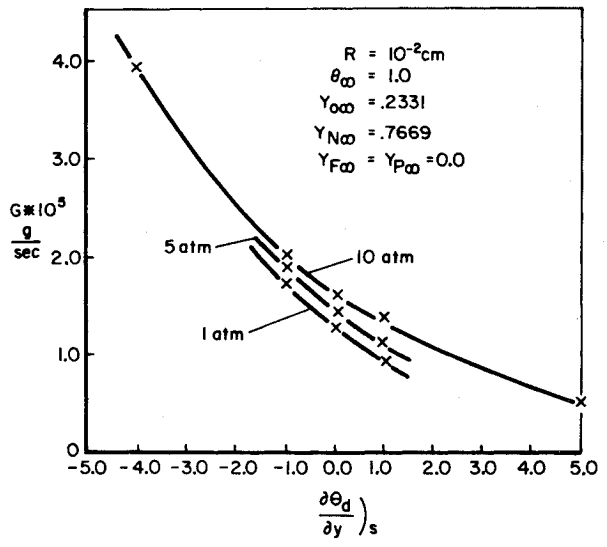

Fig. 3 Function S_1 for decane when the pressure varies.

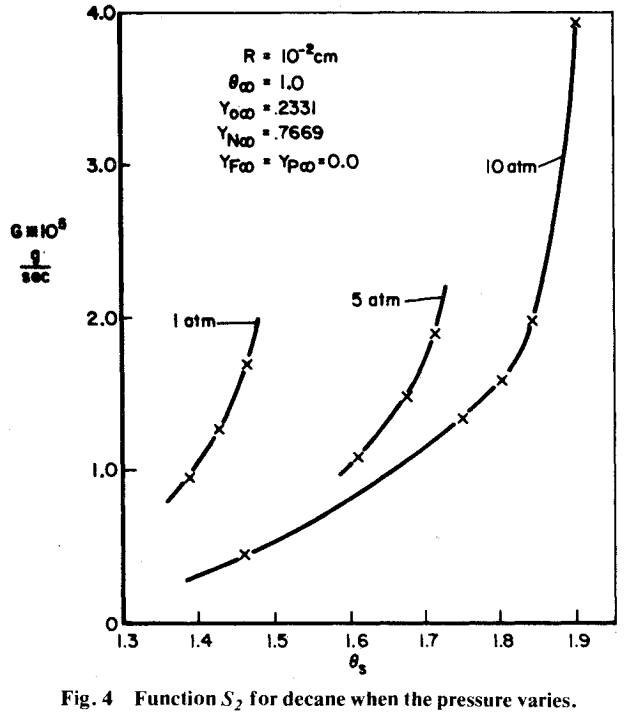

Fig. 4 Function S_2 for decane when the pressure varies.

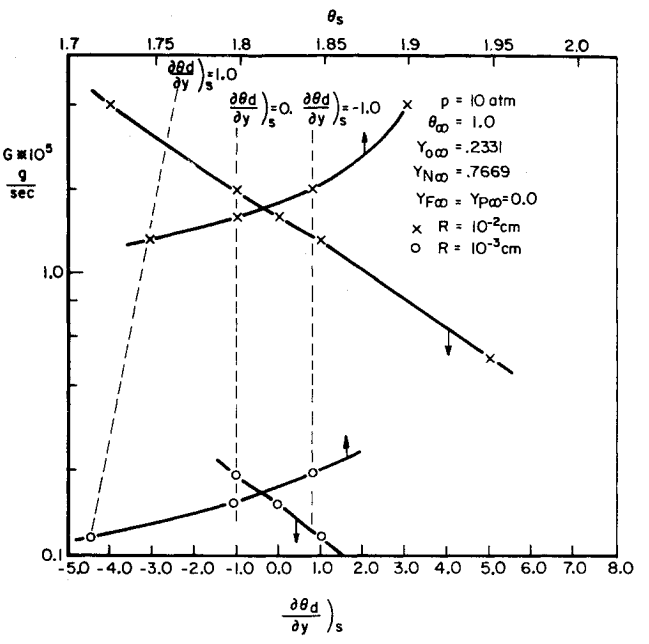

Fig. 5 Functions S_1 and S_2 for decane when the radius of the droplet varies.

was not losing heat), θ_s is larger accordingly. As θ_s is higher, so is G. It follows that Y_{Fs} is larger while Y_{Os}, Y_{Ns}, and Y_{Ps} are lower. For a given p, the minimum $(\partial\theta_d/\partial y)_s$ which would correspond to a steady-state solution in the liquid phase is that obtained for $\theta_s = \theta_b$. (Note that during a dynamic burning of the droplet, for example, when the ambient pressure has a variation which is imposed by external factors, θ_s could possibly be larger than θ_b, and, consequently, smaller values of $(\partial\theta_d/\partial y)_s$ could exist. However, these particular quasi-steady solutions of the gas field cannot be found from the experiments suggested in the previous section.) Because $(d\theta_g/dy)_s$ is always positive, $(\partial\theta_d(\partial y)_s$ must satisfy the following relationship

$$\left[-\frac{\partial\theta_d}{\partial y}\right)_s\right]\frac{\lambda_d R T_{\text{ref}}}{Q_s} < G$$

For each choice of a negative value for $(\partial\theta_d/\partial y)_s$ the previous expression provides a lower limit on G and thus on θ_s. If this lower limit gives $\theta_s > \theta_b$, there is no possible steady-state solution in the liquid phase which would be coupled to a quasi-steady solution in the gas phase. This limit is heavily dependent on Q_s (for fixed R). As $(\partial\theta_d/\partial y)_s$ decreases while being negative, $(d\theta_g/dy)_s$ decreases approaching zero.

Whenever $(\partial\theta_d/\partial y)_s$ is positive, the droplet is cool enough so that it needs to absorb heat from the gas phase. As a consequence, θ_s is lower than in the case when $(\partial\theta_d/\partial y)_s = 0$. The results show that as $(\partial\theta_d/\partial y)_s$ increases, θ_s decreases. Then G is smaller and so is Y_{Fs}, whereas Y_{Os}, Y_{Ns}, and Y_{Ps} are larger. In the process, $(d\theta_g/dy)_s$ increases approaching the slope corresponding to an angle of 90°.

Table 1 also indicates that the flame becomes thicker as $(\partial\theta_d/\partial y)_s$ increases. For large and positive $(\partial\theta_d/\partial y)_s$, θ_s is well below θ_b showing that the frequently used approximation $\theta_s \simeq \theta_b$ would be incorrect. This result is in agreement with that published earlier by Williams.[17]

As $(\partial\theta_d/\partial y)_s$ is lower, the approximation $\theta_s \simeq \theta_b$ is better and in the limit, for the lowest value of $(\partial\theta_d/\partial y)_s$ obtained for a steady-state solution in the droplet, the results of the flame sheet model are recovered.

Parametric Study

The multidimensional graphs representing S_1 and S_2 can be obtained via a parametric numerical study.

Variation of p. The results obtained at different pressures, for a fixed $(\partial\theta_d/\partial y)_s$, show that, as the pressure decreases, G and Y_{Fs} decrease, whereas Y_{Os}, Y_{Ns}, Y_{Ps} and $(d\theta_g/dy)_s$ increase. Thus, the flame becomes thicker as the pressure drops.

Variation of R. The theory using the thin-flame assumption predicts that the only dependence of the solution on R is through the ratio $GC_{pg}/\lambda_g R$.[9] Consequently, when R is varied, G will change proportionally so that the previous ratio is kept constant, whereas the quantities θ_s, Y_{Fs}, Y_{Os}, Y_{Ps}, Y_{Ns}, and $(d\theta_g/dy)_s$ remain constant. The following shows that these conclusions are too simplistic.

The results obtained by varying R are presented in Fig. 5. They show that as R decreases by an order of magnitude G decreases by more than an order of magnitude. The deviation from the classical theory is larger as θ_s decreases. By far the most important consequence of this deviation is the result that as R decreases the flame becomes thicker, an outcome which the classical flame sheet theory cannot predict. For $(\partial\theta_d/\partial y)_s = 0$, Y_{Os} varies by a factor of 10^3 when R varies from 10^{-2} to 10^{-3} cm. The present theory can predict, for instance, that it

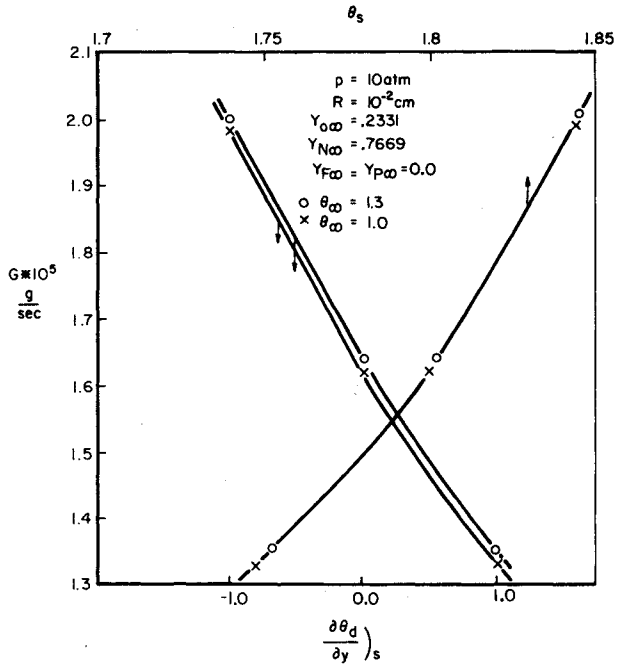

Fig. 6 Functions S_1 and S_2 for decane when θ_∞ varies.

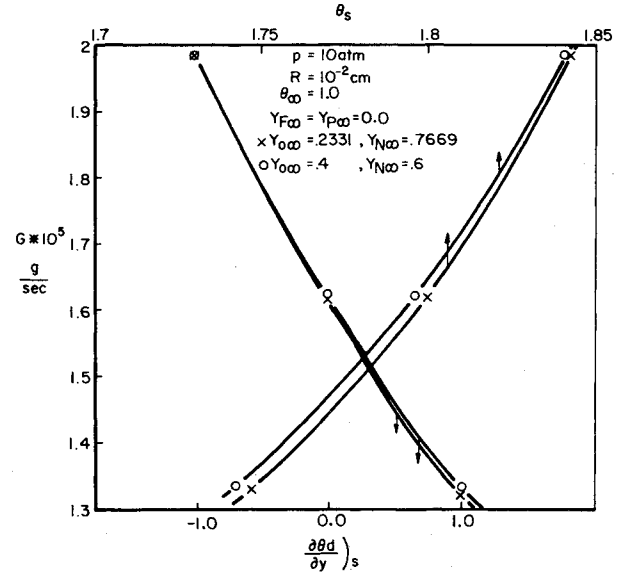

Fig. 7 Functions S_1 and S_2 for decane when $Y_{O\infty}$ and $Y_{N\infty}$ vary.

is easier to extinguish a smaller droplet than a larger one. This is a well-known experimental fact.

For a fixed $(\partial\theta_d/\partial y)_s$, as R decreases by an order of magnitude, θ_s decreases, which accounts for a larger than expected decrease of G, a decrease of Y_{Fs}, a larger increase of Y_{Os} and a slight increase of Y_{Ps} and Y_{Ns}. The value of $(d\theta_g/dy)_s$ decreases, indicating that less heat from the gas phase is fed back to the droplet.

Variation of θ_∞. Figure 6 shows the results obtained when θ_∞ is 1.3 instead of 1. It can be seen that when $(\partial\theta_d/\partial y)_s$ is fixed, G and θ_s increase slightly with respect to the reference case. This is in agreement with the trends expected from the classical theory.[9] However, what the thin-flame theory cannot anticipate is that the flame is now thinner, indicating, for instance, that it is more difficult to extinguish a droplet as the ambient temperature is higher.

While Y_{Fs} is slightly higher than in the reference case, both Y_{Ps} and Y_{Ns} are slightly lower. Also, for the same $(\partial\theta_d/\partial y)_s$, the value of $(d\theta_g/dy)_s$ increases suggesting that more heat is passed to the droplet from the gas phase.

Variation of $Y_{O\infty}$ *and* $Y_{N\infty}$. The results obtained by increasing $Y_{O\infty}$ and decreasing $Y_{N\infty}$ are plotted in Fig. 7. They show that for a fixed $(\partial\theta_d/\partial y)_s$, G increases slightly, an outcome anticipated by the classical theory.[9] However, what could not be predicted by previous theories is that θ_s and Y_{Fs} may both decrease as has happened in this case. This explains why the increase in the value of G is so slight; whereas decreasing Y_{Fs} tends to increase G, the decrease of θ_s tends to decrease G. These two phenomena are taken into account by the Langmuir-Knudsen law. Notice that both the decrease of Y_{Fs} and the increase of $(d\theta_g/dy)_s$ are consistent with the fact that the region of highest temperature is now closer to the droplet surface than in the reference case. Another interesting observation concerns the thickness of the flame; the flame now is considerably thinner (the ratio of Y_{Os}'s is about 10^3) indicating, for instance, that it would be more difficult to extinguish a droplet in the present conditions. Because Y_{Fs}, Y_{Os}, and Y_{Ns} have all lower values than in the reference case, Y_{Ps} is larger.

Variation of $Y_{F\infty}$ *and* $Y_{P\infty}$. Thus far, $Y_{F\infty}$ and $Y_{P\infty}$ were kept constant. In order to determine how the functions S_1 and S_2 depend on the variables, two calculations were made for different values of $Y_{F\infty}$ and $Y_{P\infty}$. The results of these calculations were not plotted because they are very similar to those of Fig. 7.

The first calculation was made for an ambient atmosphere composed of gaseous fuel and air but no combustion products ($Y_{F\infty}=0.05$, $Y_{O\infty}=0.2214$, $Y_{N\infty}=0.7286$, $Y_{P\infty}=0$), whereas the second calculation was made for an ambient atmosphere composed of combustion products and air but no gaseous fuel ($Y_{P\infty}=0.05$, $Y_{O\infty}=0.2214$, $Y_{N\infty}=0.7286$, $Y_{F\infty}=0$). The remaining parameters were the same as for the reference case presented in Table 1.

For a fixed $(\partial\theta_d/\partial y)_s$, in both calculations, the value of G decreased very slightly with respect to the reference case as predicted by the classical theory, while the values of θ_s and Y_{Fs} both increased. This increase was more significant when gaseous fuel was present in the ambient atmosphere. It was also found that the value of $(d\theta_g/dy)_s$ decreased with respect to the reference case; this decrease was more important when combustion products were present in the ambient atmosphere. In both calculations, the value of Y_{Ns} was lower than in the reference case. The main difference between these two sets of results was the following: the flame was thinner than in the reference case when fuel existed in the ambient atmosphere, whereas the flame was thicker when combustion products were present in the ambient atmosphere. In addition, Y_{Ps} decreased in the former case but increased in the latter case.

Comments on the Usefulness of the Experiments

Since it has been proposed earlier in this paper to obtain the functions S_1 and S_2 from experiments, it is now sought, in the light of the numerical results, to investigate what the maximum range is for which experiments can be used to determine the graphs in Figs. 3 and 4. This range will be limited on one side by $T_d(r=0)=0°K$, and on the other by a value for $T_d(r=0)$ just below the boiling point at the pressure chosen to perform the experiments.

The results presented in Table 1 show that for $(\partial\theta_d/\partial y)_s=0$, $\theta_d(y=0)=1.79935$ which is an easily attainable temperature. However, if $\theta_d(y=0)$ is computed for $(\partial\theta_d/\partial y)_s=5$ and $(\partial\theta_d/\partial y)_s=-1$, one finds, respectively, -4.37 and 2.13. The first number indicates that a negative temperature, in degrees Kelvin, is needed to obtain the results for $(\partial\theta_d/\partial y)_s=5$, and the second number shows that the temperature at the center of the droplet should be above the boiling point at 10 atm in order to obtain the particular set of results for $(\partial\theta_d/\partial y)_s=-1$. The first condition is impossible; the second condition lies outside of the range described by this model.

Table 2 Δr_{min} using $|\Delta T|/T_\infty \sim 0.1$

$R_{(cm)}$	$\partial\theta_d/\partial y_s$					
	-5	-1	1	5	10	100
10^{-2}	0.2×10^{-3}	10^{-3}	10^{-3}	0.2×10^{-3}	10^{-4}	10^{-5}
10^{-1}	0.2×10^{-2}	10^{-2}	10^{-2}	0.2×10^{-2}	10^{-3}	10^{-4}
1	0.2×10^{-1}	10^{-1}	10^{-1}	0.2×10^{-1}	10^{-1}	10^{-3}

This simple calculation shows that, in the case of decane, there is a restricted range for which the experiments can provide the information desired to determine the functions S_1 and S_2. However, this range is of interest for many problems.

Conclusions

A way of studying the unsteady combustion of droplets has been presented. This method has several advantages. The computations in the case of an unsteady burning droplet can be reduced to the integration of one nonlinear partial differential equation, namely the energy equation for the droplet. The information about the fuel characteristics, chemical kinetics, and thermal properties is all contained in a boundary condition (represented by two functions) for which numerical values can be determined from droplet experiments.

A multidimensional graph obtained by numerical means illustrates the two functions for decane. For a fixed pressure, solutions are found for both $(\partial\theta_d/\partial y)_s$ negative and positive. In the limit of large negative values of $(\partial\theta_d/\partial y)_s$ corresponding to steady-state solutions in the droplet, the quasi-steady solution in the gas field approaches the classical flame-sheet solution with surface temperatures very close to the boiling point. For large positive values of $(\partial\theta_d/\partial y)_s$ quasi-steady solutions may exist with surface temperatures much lower than the boiling point. The pressure dependence shows an increase in the flame thickness as the pressure drops. Thicker flames are also predicted for decreasing droplet radii, lower ambient temperatures, smaller amounts of oxygen or fuel, or larger quantities of products in the ambient gas.

Appendix A: Thermocouple Measurements of T_s

The measurement of a surface temperature is not a trivial one. Therefore, it is felt that a discussion is necessary for appreciating the errors introduced in the determination of F_1 and F_2 via this measurement. However, one should keep in mind that it is much easier to measure T_s than the chemical kinetic constants.

There are two questions to be considered: a) what temperature is the thermocouple measuring, and b) how accurate is the measurement (inaccuracies occur due to the nonsteady heat transfer from the surface of the droplet to the thermocouple, thermocouple characteristics, etc.).

Let $(\partial\theta_d/\partial y)_s = a$ be the nondimensional slope at the droplet surface on the droplet side. Then

$$\Delta r_{min} = (\Delta T/T_\infty)(R/a)$$

where Δr_{min} is the minimum thickness of the thermal layer at the droplet surface. If the thermocouple is able to accurately measure temperatures in the layer Δr_{min}, the experiment is considered satisfactory.

If $a=0$ the previous relationship is not valid, but in this simple case the temperature will be constant in a small layer and the measurement of T_s is easier. Indeed, thermocouples of 4 μ could measure T_s for a $R=10^{-2}$ cm droplet better than the value one could obtain by numerically solving a nonsteady energy equation for the droplet and using 41 points per radius.

If $a\neq 0$ consider the most unfavorable case when ΔT is large across Δr_{min}. A conservative estimate is $|\Delta T|/T_\infty \sim 0.1$. Table 2 gives Δr_{min} in cm using the previous estimate, and the discussion refers to the results obtained for decane. For $(\partial\theta_d/\partial y)_s<0$, Δr_{min} is large enough so that a 4 μ thermocouple could perform the measurement of a surface temperature. Also, as $|(\partial\theta_d/\partial y)_s|$ increases while $(\partial\theta_d/\partial y)_s<0$, T_s approaches T_b, so that the experimentalist has an intuition of what should be obtained.

For $(\partial\theta_d/\partial y)_s>0$, the situation is more complex. For $R\geq 10^{-2}$ cm and $(\partial\theta_d/\partial y)_s\leq 5$, a 4 μ thermocouple will still give a good resolution. For $(\partial\theta_d/\partial y)_s=10$ and $R=10^{-2}$ cm the thermocouple can no longer perform the measurement. As R decreases and $(\partial\theta_d/\partial y)_s$ increases, the situation becomes worse. This is to say that measurements become more difficult as T_s becomes smaller.

It should be possible to measure T_s for droplets down to a 100 μ radius; however, for droplets smaller than 500 μ this measurement becomes quite difficult and for droplets in the range 100-200 μ the measurement is at the limit of the standard thermocouple techniques. In general, a thermocouple with very good characteristics will measure temperatures with a maximum accuracy of about 0.5°K.

From the numerical results obtained with decane, it can be concluded that, even though the prediction of G and Y_{Fs} could be still considered adequate for such a variation in T_s (this depends on the problem to be solved using F_1 and F_2), the thickness of the flame, which is indicated by the magnitude of Y_{Os}, could be considerably inaccurate. However, only the values of G and T_s must be determined experimentally in order to obtain F_1 and F_2. For this reason, the measurement of T_s with a thermocouple can be considered good enough for a large number of problems.

Appendix B: Criterion for Recognizing a Quasi-Steady Gas Phase Solution

For any value of G, the set of Eqs. (19-30) can be solved numerically, and a mathematical solution is obtained. However, these equations give a physical solution only for a single value of G. The criterion used for recognizing the physical solution is obtained by integrating the conservation equations and computing the ratio of those integrals. Then, the quasi-steady solution must satisfy

$$\frac{(Y_F - Y_{Fs}) - \dfrac{\lambda_g R}{GC_{pg}}\left[\left(y^2\dfrac{dY_F}{dy}\right) - \dfrac{dY_F}{dy}\right)_s\Bigg]}{(Y_O - Y_{Os}) - \dfrac{\lambda_g R}{GC_{pg}}\left[\left(y^2\dfrac{dY_O}{dy}\right) - \dfrac{dY_O}{dy}\right)_s\Bigg]} = c_1$$

$$\frac{(\theta_g - \theta_s) - \dfrac{\lambda_g R}{GC_{pg}}\left[\left(y^2\dfrac{d\theta_g}{dy}\right) - \dfrac{d\theta_g}{dy}\right)_s\Bigg]}{(Y_F - Y_{Fs}) - \dfrac{\lambda_g R}{GC_{pg}}\left[\left(y^2\dfrac{dY_F}{dy}\right) - \dfrac{dY_F}{dy}\right)_s\Bigg]} = -\frac{C}{C_{pg}T_{ref}}\frac{1}{c_1}$$

These ratios are computed in the far field. If these relationships are not satisfied, a new guess is made for G and the computation starts again.

Note: The solution obtained for $R=10^{-2}$ cm, $p=10$ atm, $\theta_\infty=1$, $Y_{O\infty}=0.2331$, $Y_{N\infty}=0.7669$, $Y_{F\infty}=Y_{P\infty}=0$ and $(\partial\theta_d/\partial y)_s=0$ had A (instead of G) as eigenvalue.

Acknowledgments

This research was sponsored by the Office of Naval Research Contract N0014-75-C-0705. One of the authors (J.B.) would like to acknowledge Dr. F. Bracco, Princeton University, for some useful information.

References

[1]Kumagai, S., Sakai, T., and Okajima, S., "Combustion of Free Fuel Droplets in a Freely Falling Chamber," *Proceedings of 13th Symposium on Combustion*, The Combustion Institute, Pittsburgh, Pa., 1971, pp. 779-785.

[2]Krier, H. and Wronkiewicz, J. A., "Combustion of Single Drops of Fuel," *Combustion and Flame*, Vol. 18, 1972, pp. 159-166.

[3]Spalding, D. B., "Theory of Particle Combustion at High Pressures," *Journal of the American Rocket Society*, Vol. 29, 1959, pp. 828-835.

[4]Strahle, W. C., "A Theoretical Study of Unsteady Droplet Burning: Transients and Periodic Solutions," Ph.D. Dissertation, Princeton University, Princeton, N.J., 1963.

[5]Chervinsky, A., "Transient Burning of Spherical Symmetric Fuel Droplets," *Israel Journal of Technology*, Vol. 7, No. 1-2, 1969, pp. 35-42.

[6]Kotake, S. and Okazaki, T., "Evaporation and Combustion of a Fuel Droplet," *International Journal of Heat and Mass Transfer*, Vol. 12, 1969, pp. 595-609.

[7]Hubbard, G. L., Denny, V. E., and Mills, A. F., "Droplet Evaporation: Effects of Transients and Variable Properties," *International Journal of Heat and Mass Transfer*, Vol. 18, 1975, pp. 1003-1008.

[8]Nuruzzman, A. S. M. and Beer, J. M., "On the Non-Steady State Nature of Droplet Combustion," *Combustion Science and Technology*, Vol. 3, 1971, pp. 17-24.

[9]Williams, F. A., *Combustion Theory*, Addison-Wesley, Reading, Mass., 1965.

[10]Tarifa, C. S., del Notario, P. P., and Moreno, F. G., "Combustion of Liquid Monopropellants and Bipropellants in Droplets," *Proceedings of 8th Symposium International on Combustion*, Williams and Wilkens Co., Baltimore, Md., 1960, pp. 1035-1056.

[11]Zeldovich, Ya. B., "On the Theory of Burning of Powders and Explosives," *Journal of Experimental and Theoretical Physics*, Vol. 12, No. 11-12, 1942, pp. 498-524.

[12]Summerfield, M., Caveny, L. H., Battista, R. A., Kubota, N., Gostintsev, Yu., A., and Isoda, H., "Theory of Dynamic Extinguishment of Solid Propellants with Special Reference to Nonsteady Heat Feedback Law," *Journal of Spacecraft and Rockets*, Vol. 8, Aug. 1971, pp. 251-258.

[13]Bellan, J. and Summerfield, M., "On the Quasi-Steady Gas Phase Assumption for a Burning Droplet," to be published in *AIAA Journal*.

[14]Lorell, J., Wise, H., and Carr, R. E., "Steady-State Burning of a Liquid Droplet. II. Bipropellant Flame," *Journal of Chemical Physics*, Vol. 25, No. 2, 1956, pp. 325-331.

[15]Bracco, F. V., "Nitric Oxide Formation in Droplet Diffusion Flames," *Proceedings of 14th Symposium International on Combustion*, The Combustion Institute, Pittsburgh, Pa., 1972, pp. 831-842.

[16]*Petroleum Refining*, American Petroleum Institute, Division of Refining, New York, 1966.

[17]Williams, F. A., "On the Assumptions Underlying Droplet Vaporization and Combustion Theories," *Journal of Chemical Physics*, Vol. 33, No. 1, 1960, pp. 133-144.